Catalysis Science & Technology

ROYAL SOCIETY OF CHEMISTRY

PAPER

View Article Online
View Journal | View Issue



Cite this: *Catal. Sci. Technol.*, 2025, **15**, 3354

# Tuning formate surface coverage with cosolvents for liquid-phase catalytic transfer hydrogenation†

Ezra A. Baghdady, J. Will Medlin * and Daniel K. Schwartz *

The synergistic effects of cosolvent and hydrogen-donor (formate) concentration on Pd-catalyzed transfer hydrogenation of vinylphenol are explored for water and water–alcohol mixtures, with a change in the optimum cosolvent mixture observed for different formate concentrations. The results are interpreted in terms of solvent-based tuning of the formate surface coverage, where an optimal formate coverage is required to facilitate hydrogen transfer without excessively blocking surface binding sites. This interpretation is supported by measurements of the formate surface coverage using adsorption-induced attenuation of self-diffusiophoretic Janus particle motion in water and a water–alcohol solvent. The adsorption isotherms demonstrated tuning of formate surface coverage by the cosolvent, with addition of the alcohol cosolvent increasing formate adsorption. The results contribute to rational solvent selection for transfer hydrogenation reactions and provide insight into the roles cosolvents can play in the design of liquid-phase catalytic reaction systems.

Received 19th October 2024,
Accepted 23rd April 2025

DOI: 10.1039/d4cy01254b

rsc.li/catalysis



## Introduction

Though molecular hydrogen has remained the reductant of choice for catalytic hydrogenation reactions for many years, the need for sustainable chemical production has spurred interest in utilizing hydrogen stored in liquid carriers for safe, high density storage and transport and reduced pressure requirements for reactor design.[1] Of the hydrogen carriers of interest, formate salts and formic acid have emerged as attractive reductants due to the ease of handling either the solid (formate salts) or liquid (formate salt and formic acid solutions), high hydrogen storage capacity, and the benign dehydrogenation product (carbon dioxide), which can be electrochemically recycled to formate in an atom-efficient cycle.[2,3] Of interest in fuel and commodity chemical production from lignocellulosic biomass is transfer hydrogenation of the highly functionalized and reactive bio-oils produced by pyrolysis or hydrothermal liquefaction to generate stable chemical species.[4,5] As both lignin and raw bio-oil are poorly soluble in water, a low cost cosolvent such as an alcohol is often added (or used alone) to solubilize the material.[6] The presence of such cosolvents can impact transfer hydrogenation reactions for several reasons, including transition state (de)stabilization[7] and competition with reactants for active sites.[8] While each of these mechanisms can affect activity, solvent–solute interactions have also been shown to modify reagent adsorption to the catalyst surface,[9,10] which potentially enables tuning of reaction activity by control of formate coverage. Because formate adsorbs strongly to catalyst surfaces[11,12] and also interacts strongly with solvents (*e.g.* through hydrogen-bonding),[13] we hypothesized that the steady-state coverage, and therefore reaction rate, of catalytic transfer hydrogenation utilizing formate could be "tuned" by changing the nature of the solvent mixture.

At low formate concentration, a deficiency of surface-bound hydrogen donor will necessarily result in low transfer hydrogenation rate, with activity approaching zero as formate coverage approaches zero. On the other hand, formate is known to inhibit the transfer hydrogenation reaction at high concentration *via* competitive adsorption.[14] In other words, transfer hydrogenation with formate at "low" concentration is expected to be positive order in formate, while at "high" concentration, competitive adsorption between formate and the substrate is expected to result in negative order in formate. "Low" and "high" concentration in this work are relative to the concentration at which activity is maximized with respect to formate concentration. Formate adsorption therefore plays an important role in the transfer hydrogenation reaction. Transfer

*Chemical and Biological Engineering, University of Colorado Boulder, UCB 596, Boulder, Colorado 80309, USA. E-mail: ezra.baghdady@colorado.edu, will.medlin@colorado.edu, daniel.schwartz@colorado.edu*

† Electronic supplementary information (ESI) available: Schematic of imaging cell assembly, MSDs and fits for diffusive particle motion in water and 20% IPA, fitted concentration profiles for the transfer hydrogenation reactions, fitted initial reaction rates for the transfer hydrogenation reactions, apparent coverage and linearized isotherms for formate adsorption onto Pd-based active particles, linearized isotherms for formate adsorption onto Pt-based active particles, drift velocity of active particles in varying concentrations of IPA, and gas chromatography method parameters. See DOI: https://doi.org/10.1039/d4cy01254b

hydrogenation rates are expected to be low due to low formate coverages at low formate concentration, while they are expected to be suppressed by competitive adsorption at high formate concentration. The optimum formate coverage is therefore intermediate; high enough to yield an appreciable rate of hydrogen transfer, but low enough to avoid competition with other substrates.

We report a combined study probing the synergistic effects of solvent composition and formate concentration on catalytic transfer hydrogenation of vinylphenol. We first show that, at low formate concentrations, the addition of an alcohol cosolvent enhanced the transfer hydrogenation reaction rate over a Pd catalyst, while at high formate concentration the cosolvent caused inhibition of the reaction. The results are explained in terms of solvent effects on the steady-state surface coverage of formate as function of a formate activity coefficient, which encoded the solvent effect on formate activity. Next, we quantitatively probed formate adsorption onto a proxy Pt catalyst surface utilizing a technique developed by our lab to measure molecular adsorption in liquid media *via* transport analysis of self-diffusiophoretic Janus particle dynamics. Langmuir isotherms were extracted from these measurements that show formate adsorption was increased in the presence of the alcohol cosolvent. The results inform the design of catalytic transfer hydrogenation systems based on formates and, more generally, provide insight to the capability of cosolvents to "tune" liquid-phase catalytic reactions by control of reagent surface coverage.

## Materials and methods

### Materials

The 5 wt% Pd/silica (reduced, dry, Escat 1351 silica) was purchased from Sigma Aldrich. Potassium formate was purchased from Oakwood Chemical (N. Estill, SC). Borosilicate glass coverslips (24 × 30 mm, #1.5) were purchased from Electron Microscopy Sciences. 4-Vinylphenol (10.05 wt% in propylene glycol), isopropanol (ACS plus grade), hydrogen peroxide (ACS grade, 30 wt%, stored at 4 °C), and sulfuric acid (ACS plus grade) were purchased from Fisher Chemical. Ethanol (200 proof) was purchased from Decon Labs. Anhydrous methanol (99.8%) was purchased from Thermo Scientific. Water (HPLC grade) was purchased from Macron Fine Chemicals. HPLC grade water was used in all experiments unless otherwise noted.

### Transfer hydrogenation reaction study

Solutions of 20 mM vinylphenol were prepared in water, a 10 mol%, and a 20 mol% isopropyl alcohol/water cosolvent mixture. Methanol was added to each mixture as an internal standard at a concentration of 0.7 M. Reactions were performed in a 100 mL liquid phase batch reactor (Parr Instrument Co., Moline IL) equipped with a borosilicate glass liner at 75 °C under a 100 psi nitrogen atmosphere at a stir rate of 900 rpm. The reaction solution contained 33.25 mL of the vinylphenol solution, 60 mg of Pd/silica catalyst, and either potassium formate solution or solid weighed out to yield formate concentrations ranging from 10 mM to 4 M. The reactor was sampled at time points of 0, 5, 10, 15, 20, and 30 minutes throughout the reaction, with samples immediately passed through a 0.22 μm syringe filter to remove the catalyst. The samples were transferred to amber glass vials and analyzed using an Agilent 7890A gas chromatograph equipped with an Agilent HP-5 capillary column (Table S1†).

### Modeling of reaction results

The reaction was modeled using a modified Langmuir–Hinshelwood expression described by Wang and Wang:[15]

$$r = \frac{k(K_A\gamma_A C_A)^n K_B\gamma_B C_B}{\left(1 + (K_A\gamma_A C_A)^n + K_B\gamma_B C_B\right)^2} \cong \frac{kK_B C_B (K_A\gamma_A C_A)^n}{\left(1 + (K_A\gamma_A C_A)^n\right)^2} \quad (1)$$

Here, the A and B subscripts refer to formate and 4-vinylphenol, respectively, $r$ represents the initial reaction rate (mM $g^{-1}$ $s^{-1}$), $k$ represents the rate constant (mM $g^{-1}$ $s^{-1}$), $K$ represents the adsorption equilibrium constant ($mM^{-1}$), $\gamma$ represents the (unitless) activity coefficient of the dissolved species, and $C$ represents species concentration. Cooperative formate adsorption to Pd was described using a Hill coefficient $n$, which, when set to 1, reduces the equation to the Langmuir–Hinshelwood model. As a simplification, we assumed that the dominant non-ideality present was that of the cosolvent on formate activity and neglect solvent effects on the vinylphenol activity coefficient. This allowed us to fix $\gamma_B$ at unity to obtain a tractable number of fitted parameters. Under almost all reaction conditions, the formate concentration was many times greater than that of the substrate, therefore we neglected the substrate coverage term in the denominator. The transfer hydrogenation data were fitted by the model in an iterative approach to estimate the effect of the cosolvent on the formate activity coefficient. First, the model was fitted to the water solvent data to estimate $K_A$ and $kK_B$ (grouped as a constant) while holding $\gamma_A$ at unity. Next, the model was fitted to the 10 and 20 mol% IPA solvent data, holding $K_A$ constant at the value determined in the water solvent to estimate the formate activity coefficient as a function of the solvent composition. Unless otherwise indicated, all reported error estimates represent either the standard error of the mean (s.e.m.) or the standard error of the fitted value.

### Active particle synthesis

Fluorescent polystyrene microspheres (Sigma Aldrich, 1 μm, 2% solids, fluorescent red (580/605)) were vortex-mixed for 15 s and a 20 μL aliquot was mixed with 150 μL of a 5% isopropanol in water solution (particle dilution factor of 8.5). The isopropanol served to reduce the solution surface tension for spin-coating without largely impacting colloid stability. One 10 μL drop of the suspension was spin-coated onto 6–9 piranha-cleaned 25 mm circular coverslips using a Laurell Technologies Co. model WS-400BX-6NPP/LITE spin-coater (Lansdale, PA) for 3 minutes at 2500 rpm to deposit a sub-monolayer of particles. A

Cressington 108-auto sputter coater equipped with a Cressington mtm-10 quartz crystal microbalance (Watford, U.K.) was used to deposit a 5.0 ± 0.2 nm layer of platinum onto the sub-monolayer of particles. The sputtering process resulted in asymmetric deposition of the metal due to the self-shadowing of each spherical particle.[16] The Janus particles were released from the coverslips by bath sonication into 6 mL of water for 2 min each. The Janus particle dispersion was further diluted by a factor of 2–3 to optimize the number of particles in the microscope field of view. The particle dispersions were stored in the dark at 4 °C to limit photobleaching.

### Piranha cleaning procedure

Coverslips were cleaned *via* immersion in a solution of 30 mL of 30 wt% hydrogen peroxide and 75 mL of sulfuric acid (ACS grade) for 45 minutes. Note: piranha solution is highly hazardous and must be handled with special safety considerations.[17] After immersion, the coverslips were washed in copious amounts of deionized water and dried in a stream of high-purity nitrogen (AirGas).

### Imaging cell preparation

Stock solutions of potassium formate were prepared in water and in a mixture of IPA and water such that the final imaging concentration was 0 mol% IPA or 20 mol% IPA. The as-synthesized Janus particles were redispersed *via* bath sonication for 20 minutes and 50 μL of stock potassium formate solution was pipette-mixed with 100 μL of the particle solution and allowed to equilibrate for one hour. To prepare an imaging cell, 10 μL of 30 wt% hydrogen peroxide was pipette-mixed with 40 μL of the particle–solute solution and a 3 μL drop was deposited onto a piranha-cleaned coverslip. A 9 mm × 0.5 mm silicone perfusion chamber (Invitrogen CoverWell) was fixed over the droplet and depressed such that the droplet formed a capillary bridge between the top and bottom of the cell. An 18 × 18 mm coverslip was placed on the top of the cell to better isolate the system from the environment and prevent evaporation (Fig. S1†). Formate adsorption isotherms were collected in the absence of any organic (*i.e.*, vinylphenol) other than the IPA cosolvent. This was due to previous observation of interference due to organics that react homogeneously with the hydrogen peroxide fuel.[16] These reactions can both affect particle motion and generate more strongly binding species such as aldehydes, convoluting the results.

### Particle imaging and data analysis

Imaging was performed on a Nikon Ti-E microscope equipped with a Hamamatsu ORCA-Flash4.0 V2 C11440 camera using a 100× oil-immersion objective with fluorescence excitation at 561 nm. Videos were acquired at a frame rate of 100 frames per second for at least 900 frames. The videos were acquired over multiple fields of view to obtain trajectories of a representative sample of particles. Each imaging cell was imaged for no more than 20 minutes to ensure that any changes in the hydrogen peroxide fuel concentration or surface oxidation state of the as-sputtered (metallic) Pt (ref. 18) remained minimal. Observation of consistent particle velocity over the course of each experiment indicated minimal change in either fuel concentration or Pt oxidation state[19] occurred for a given experiment.

Particle trajectories were extracted from the videos using custom MATLAB software and particle dynamics were quantified by determining the time-averaged two-dimensional mean-squared displacement (MSD) for each trajectory. The 2D MSD was calculated from the particle trajectories by

$$\langle r^2 \rangle = \frac{1}{N}\sum_{1}^{N} |r(t_0 + \Delta t) - r(t_0)|^2 \quad (2)$$

where $\langle r^2 \rangle$ represents the mean-squared displacement, $N$ represents the number of frames in a given trajectory and $r$ represents the 2D geometric displacement of the particle between times $t_0$ and $t_0 + \Delta t$. For short lag time $\Delta t$ relative to the rotational diffusion timescale (*i.e.*, the ballistic regime[20]), the mean-squared displacement was modeled using the expression

$$\langle r^2 \rangle = 4D_T\Delta t + V^2\Delta t^2 \quad (3)$$

where $D_T$ represents the particle translational diffusion coefficient and $V$ represents the drift velocity.[20] Only the first ten points of the experimental MSDs (corresponding to a maximum lag time of 0.1 s) were fitted in order to extract the drift velocity using data associated with timescales well below the characteristic rotational diffusion time.

The translational diffusion coefficients of the active particles were determined by calculating the MSDs of particles undergoing diffusive motion (*i.e.*, no fuel present) in water and in 20 mol% IPA and fitting the MSDs by eqn (3) with $V$ equal to zero (Fig. S2†). Particle drift velocity was extracted by fitting the MSDs of particles undergoing active motion with eqn (3) using the obtained diffusion coefficients for each solvent condition.

The attenuation of particle drift velocity in the presence of formate was attributed to the blockage of catalytic active sites for the hydrogen peroxide fuel decomposition.[21] In this manner, the apparent coverage of the adsorbed formate $\theta$ could be extracted by transforming the attenuation of particle drift velocity at a given formate concentration ($V$) relative to the drift velocity in the absence of formate ($V_0$) as follows:

$$\theta = 1 - \frac{V}{V_0} \quad (4)$$

The presence of the IPA cosolvent increased the solution viscosity, changing active particle transport. We therefore determined the drift velocity of active particles in both water and 20 mol% IPA. These measurements provided $V_0$ for each isotherm fit which corrected for changes in viscosity due to the presence of the cosolvent. Potassium formate can further perturb the viscosity, however the low salt concentrations used (≤10 mM) preempted this concern.[22]

 

The apparent coverage in water as a function of formate concentration was then fitted by a Langmuir isotherm to extract the affinity $K$ and maximum coverage $\theta_{max}$ terms. We modeled the effect of the solvent on formate activity using an apparent activity coefficient $\gamma$, defined as unity in the water solvent:

$$\theta = \theta_{max}\frac{K\gamma C}{1 + K\gamma C} \quad (5)$$

To quantify the effect of the cosolvent on formate activity, we first fit the data collected in the water solvent while holding $\gamma$ = 1. Next, the obtained affinity was used to determine the activity coefficient and maximum coverage for the apparent coverage in 20 mol% IPA.

## Results

### Transfer hydrogenation reaction study

Batch-wise vinylphenol transfer hydrogenation reactions utilizing 10, 100, 250, 500, 1000, and 4000 ppm potassium formate as the hydrogen source were performed in triplicate in pure water, 10 mol%, and 20 mol% IPA cosolvent mixture at 75 °C over a 5 wt% Pd/silica catalyst. The reaction mixture was sampled throughout the reaction to determine the rate of generation of the transfer hydrogenation product, ethylphenol (Fig. S3 and S4†). No ring or hydroxyl group hydrogenation was detected. The potassium formate concentration was varied to span formate coverages from low coverage, where increasing the coverage was expected to increase the reaction rate, to high surface coverage, where increasing the formate coverage was expected to decrease the reaction rate. While the substrate coverage also likely played a role in the reaction, we chose to hold substrate concentration constant and focus on formate, as the plethora of organic species relevant to biomass upgrading makes evaluation of the organic species of limited utility compared to that of formate. Fig. 1 shows the initial transfer hydrogenation rate in water and in the alcohol-water cosolvents, varying the bulk concentration of potassium formate. The reaction rate exhibited a peak in activity with respect to formate concentration, indicative of a Langmuir–Hinshelwood type mechanism. The key observation in this work is the shift of the peak to lower formate concentration with increasing amounts of the alcohol cosolvent. Indeed, at low formate concentration (<1 M), the reaction rate in the presence of the IPA–water cosolvent was many times greater than that in water. At higher formate concentrations (>2 M), however, the reaction in the presence of the alcohol cosolvents was attenuated relative to that in water. Interestingly, a downward offset in the observed maximum reaction rate was apparent for the water case. This may be due to solvation effects on the transition state unrelated to reagent coverage, in which the local solvent structure at the catalyst surface directly affected the transition state.[7]

We hypothesized that the reaction rate dependence on the solvent may be explained by an increase in dissolved

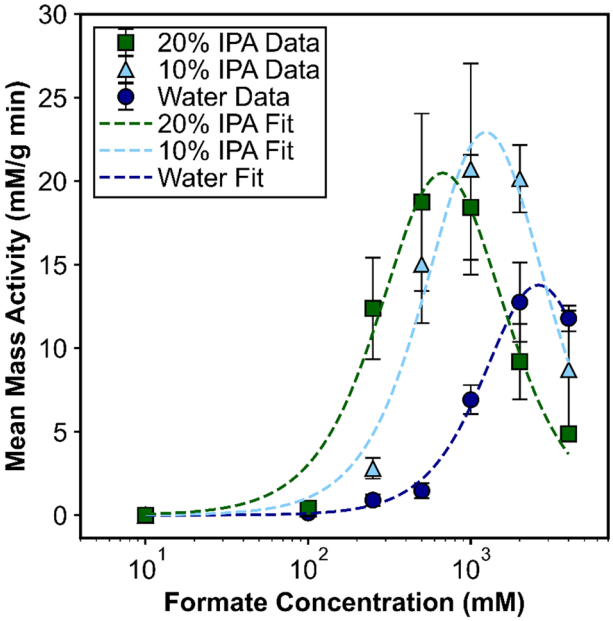


Fig. 1 Initial transfer hydrogenation rate over a Pd catalyst with potassium formate as the hydrogen source. Error bars represent standard error of triplicate reactions. At low potassium formate concentration, the reaction in the presence of the alcohol–water cosolvent exhibited enhanced activity relative to that in pure water, however at high formate concentration the reaction rate in the alcohol–water cosolvent was lower than in water. A notable shift in the optimum formate concentration for a given solvent was observed.

formate activity in the presence of the alcohol cosolvent, indicative of less-favorable solute–solvent interactions. Here, the addition of an alcohol cosolvent hypothetically results in a net destabilization of formate in solution, increasing formate adsorption to the catalyst surface. At low formate concentration, where the catalyst surface may be sparsely covered with adsorbed formate, the increase in formate surface coverage induced by the alcohol cosolvent would increase the reaction rate. At higher bulk concentrations, however, an increased formate coverage due to the cosolvent may have led to excessive blocking of sites, decreasing the reaction rate. To estimate the formate activity coefficient, the data were fitted by a Langmuir–Hinshelwood model previously described in the literature.[15] The formate activity coefficient was defined as 1 in the water solvent, with addition of 10 and 20 mol% IPA resulting in values of 2.1 ± 0.05 and 3.9 ± 0.1, respectively. Within the model, changes in the activity coefficient acted to shift the model peak to the right or left, with increased activity coefficient shifting the model peak to lower formate concentration. The Hill coefficient $n$, indicative of cooperative formate adsorption for values greater than one and descriptive of model "steepness", was estimated at values of 1.9 ± 0.04, 1.8 ± 0.06, and 1.7 ± 0.06 for increasing alcohol concentration, consistent with previous observation of cooperative adsorption between surface-bound formates.[23,24] The slight decrease in $n$ with increasing alcohol concentration may have been due to a decrease in cooperative hydrogen-

bonding interactions in response to decreased solvent polarity.

Though previous studies have demonstrated substantial solvent effects on the transfer hydrogenation rate,[25–27] direct connections between solvent environment and formate adsorption had not been experimentally probed. However, Born–Haber cycles isolating the enthalpic contributions of solvent to adsorption have substantiated solvent effects on adsorption due to both solvation and wetting/dewetting interactions.[9,28] To test the hypothesis that the effect of the cosolvent was to increase the formate coverage, we next sought to measure adsorption isotherms for formate under different solvent compositions using self-diffusiophoretic Janus particles.

### Extraction of adsorption isotherms *via* analysis of active particle dynamics

Solvents are known to affect the behavior of catalytic reactions in several ways.[29] Therefore, to probe how the cosolvent specifically affected formate adsorption onto the catalyst surface, we leveraged a technique recently developed by our lab to quantify molecular adsorption onto catalytic surfaces in liquid media *via* analysis of self-diffusiophoretic Janus particle dynamics in the presence of an adsorbate.[21] The technique relied on inhibition of the reaction driving particle self-diffusiophoresis by adsorbate occlusion of active sites. We utilized asymmetric (Janus) particles comprising a Pt hemisphere and an inert hemisphere that, in the presence of hydrogen peroxide fuel, generated a local oxygen gradient, leading to self-diffusiophoretic motion with a characteristic drift velocity $V$ (Scheme 1a). In the presence of an adsorbate, *e.g.*, formate, the self-diffusiophoretic motion is inhibited due to adsorbed formate reducing the number of Pt sites available for the fuel decomposition reaction[16] (Scheme 1b). As the bulk formate concentration is increased, the Pt surface eventually becomes saturated with adsorbed formate, completely inhibiting the self-diffusiophoresis (Scheme 1c). By measuring the drift velocity at varying formate concentrations, the apparent formate surface coverage can be quantified, as described above.

We initially attempted to utilize this technique to measure adsorption isotherms for formate on Pd based active particles, however the poor ability of Pd to catalyze the hydrogen peroxide decomposition reaction ultimately led to data with substantial experimental uncertainty (Fig. S5 and S6†). Therefore, we chose Pt as the catalytic metal for the active particle study. Formate is known to adsorb similarly onto Pd and Pt surfaces,[30] and the effect of the solvent on molecular adsorption is expected to be similar across both metals,[9] therefore we present the results for formate adsorption onto a Pt surface in both water and a 20% IPA cosolvent to demonstrate the solvent effect on adsorption, with the caveat that the two surfaces are not identical. While extraction of coverage data on the platinum surface proxy revealed promising quantitative

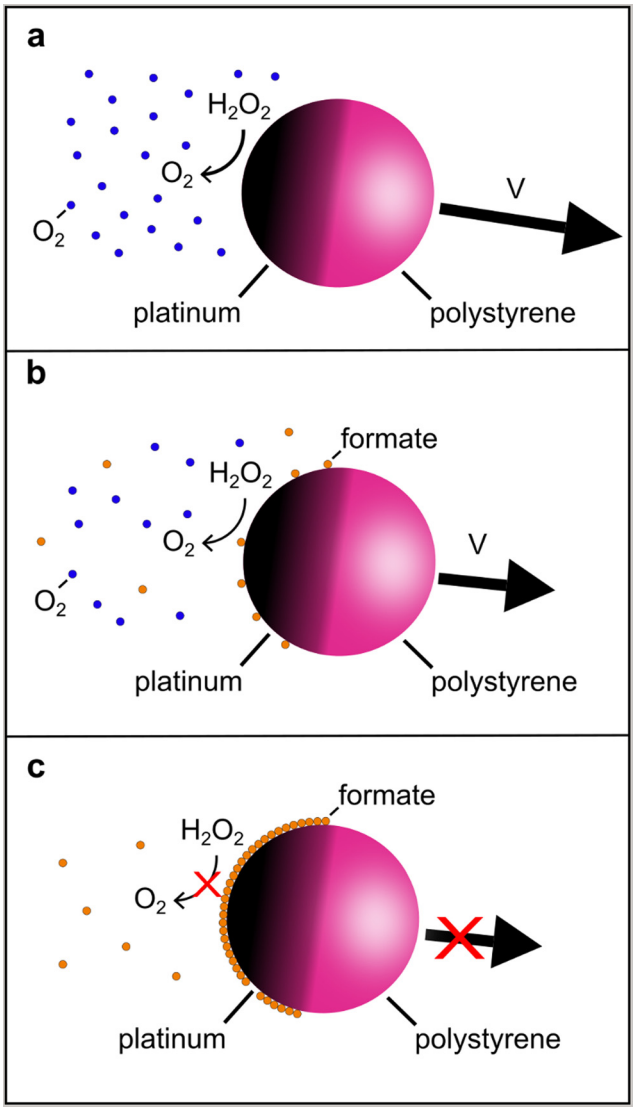


**Scheme 1** (a) Self-diffusiophoretic active particles in the presence of hydrogen peroxide exhibited a drift velocity $V$ by generation of an oxygen concentration gradient across the particle surface. (b) At low bulk formate concentration, occlusion of the Pt surface by adsorbed formate inhibited generation of the oxygen driving the self-diffusiophoresis, causing a decrease in particle velocity. (c) At high bulk formate concentration, the surface was substantially covered by formate, substantially inhibiting the self-diffusiophoretic contribution to motion.

results, direct comparison of the isotherms to the reaction conditions was challenging due to the usage of both different metals (Pt *vs.* Pd) and temperatures (20 °C *vs.* 75 °C) between studies. While unlikely to affect the general trend of increased formate adsorption in the alcohol cosolvent, these changes are expected to influence the absolute coverage values. Additionally, the presence of the formate counterion[31–34] and/or the presence of a co-adsorbed organic species[35,36] may contribute to higher order effects on adsorption/reaction of adsorbed intermediates *via* adsorbate–adsorbate interactions or competitive adsorption.

 

### Tuning formate adsorption with cosolvent mixtures

In the absence of hydrogen peroxide, the particles exhibited diffusive motion characterized by a translational diffusion coefficient $D_T$. The translational diffusion coefficients of the particles in both water and 20 mol% IPA were determined by performing object tracking on videos of particle motion in the absence of hydrogen peroxide and calculating the mean-squared displacement (MSD). The MSDs for the diffusive particles were linear, characteristic of diffusive motion, with slopes equal to $4D_T$ (Fig. S2†). The translational diffusion coefficients for particles in water and in 20 mol% IPA were 0.360 ± 0.002 $\mu m^2\ s^{-1}$ (s.e.m) and 0.170 ± 0.004 $\mu m^2\ s^{-1}$ (s.e.m) (Fig. S2†), respectively, with lower diffusion coefficient in the presence of the IPA cosolvent due to the increased viscosity of the solvent.

In the presence of the hydrogen peroxide fuel, the particles exhibited enhanced transport by self-diffusiophoresis due to fuel decomposition on the Pt hemisphere. The additional mobility contributed to the mean-squared displacement *via* the drift velocity term and was visibly observed by an upward curvature to the MSDs in some cases (Fig. 2a and b). Particle MSDs in the presence of increasing potassium formate concentration exhibited suppressed displacement, which was attributed to occlusion of the active sites for the fuel decomposition reaction by adsorbed formate. The extracted diffusion coefficients were used to fit eqn (3) to the MSDs of particles in the presence of hydrogen peroxide to extract the drift velocity at varying potassium formate concentration. This procedure enabled isolation of particle motion due to self-diffusiophoresis from background thermal motion. The attenuation of the drift velocity in increasing formate concentration was converted to an apparent coverage, and the apparent coverages were fitted to linearized forms of the Langmuir isotherm to extract the affinity $K$, maximum coverage $\theta_{max}$, and formate activity coefficient $\gamma$ (Fig. S7†).

Extraction of the adsorption parameters from the linearized isotherms revealed a substantial solvent effect on formate adsorption to the Pt surface (Fig. 2c and S7†). In the presence of water as the solvent, formate exhibited an affinity of 22.7 ± 2.1 $mM^{-1}$ and maximum coverage of 0.87 ± 0.005, with activity coefficient defined as 1. Within the 20 mol% IPA cosolvent mixture, formate exhibited a marked increase in adsorption relative to that in pure water, with increases in both activity coefficient and maximum coverage to 2.31 ± 0.17 and 0.99 ± 0.02. This increased activity was realized within the transfer hydrogenation reaction as an increase in formate coverage on the catalyst surface. For example, at 0.1 mM formate in water the formate surface coverage on the Pt surface was ~55%, while in 20% IPA the coverage at 0.1 mM was increased to ~80%, showing that changing the solvent from pure water to 20% IPA had the same effect on surface coverage as increasing the formate concentration by 10×. The implications are clear for design of bimolecular catalytic systems, in which both reagents should occupy the surface in similar proportion. The fitted values for maximum apparent coverage trended with formate activity. While maximum coverage was expected to go to 100% at sufficiently high formate concentrations, the presence of multiple site populations with differing binding affinity for formate could explain an apparent saturation at lower concentrations for the pure water solvent. This result is consistent with our previous active particle measurements of adsorption

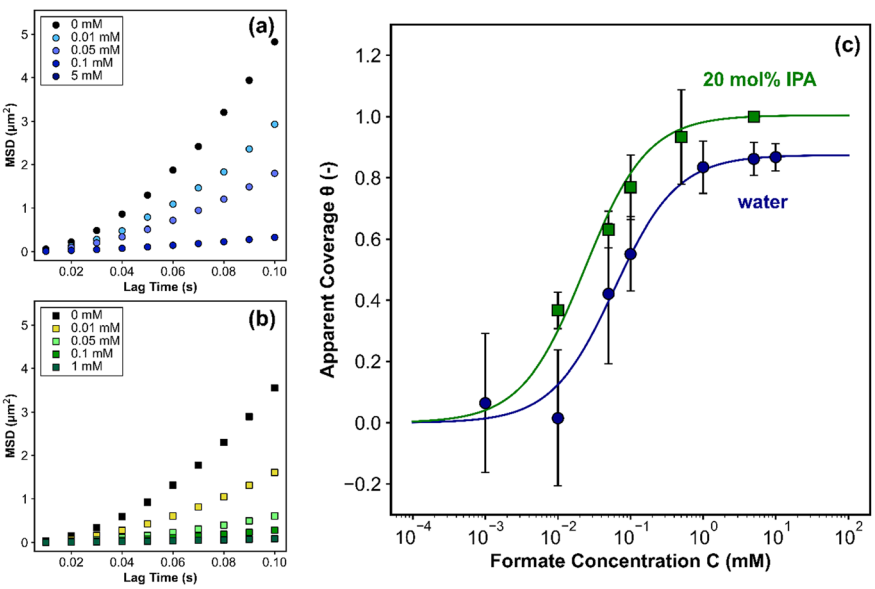


Fig. 2 Representative short time mean-squared displacements of Pt active particles in 6% hydrogen peroxide and varying concentration of potassium formate in (a) water and (b) a 20 mol% isopropyl alcohol/water solvent mixture. Experimental uncertainty (s.e.m) is on the order of the symbol size. (c) Extracted apparent coverages for formate onto platinum in water (blue circles) and 20 mol% isopropyl alcohol (green squares) with fitted Langmuir isotherms. Error bars represent propagated standard error.

isotherms: that is, we have observed that the fitted values for maximum coverage saturate at coverages below unity for all but the strongest binding adsorbates.[21]

## Discussion

When considering the thermodynamics of liquid phase adsorption, the interactions between each species must be considered, including solvent–solute, (co)solvent–surface, and solute–surface interactions, as well as other non-idealities.[37] Efforts to isolate the effect of solvent–solute interaction strength on solute adsorption enthalpy indicate that the solvent–solute interaction often contributes substantially to the adsorption enthalpy.[28] The solvent–solute interaction is therefore expected to play a dominant role in the measured differences in formate activity between the water and the alcohol–water cosolvent, as the hydrogen bond acceptor nature of the formate molecule enables strong interactions with polar solvents. Here, stronger solvent interactions between formate and water molecules serve to decrease activity relative to an organic solvent. A simplistic interpretation of the results suggests that the adsorption may be tuned based on solubility rules, given the cosolvent does not bind to the catalyst surface so strongly that it inhibits adsorption. Screening experiments with IPA suggested this was the case, as indicated by a weak response in drift velocity to IPA mole fraction (Fig. S8†). As the alcohol content was increased, the solubility of formate decreased, likely due to decreased strength of interactions between formate and the solvent (water being a stronger hydrogen bond donor than an alcohol). This caused the activity of the solvated formate to increase, as indicated by increased formate adsorption from alcohol–water mixtures. Presumably, further addition of IPA would monotonically increase dissolved formate activity and therefore formate adsorption. It must be noted that addition of IPA would also be expected to decrease the activity of the organic reactant in solution, decreasing its coverage. That effect was not explored here, in large part due to the difficulty of experimentally measuring changes in organic coverage, but future efforts could aim to fine-tune reactivity by considering such effects.

While tuning solvent composition to control the transfer hydrogenation reaction rate is certainly desirable, real biomass degradation processes generate many compounds that are sparingly soluble in aqueous media. This necessitates usage of a solvent that solubilizes both the biomass derivates and the hydrogen source for transfer hydrogenation reactions, placing a constraint on the solvent design space. As water and alcohols are typically used as (co) solvents in biomass degradation,[38,39] addition of high concentrations of a formate hydrogen source could result in transfer hydrogenation reactions unexpectedly limited by the competitive adsorption of formate and other species due to increased adsorption due to the nature of the solvent. Therefore, approaches considering the solvent effect on formate surface coverage could be implemented to recover high activity, for example, by semi-batch addition of the hydrogen donor to the reaction.

The transfer hydrogenation reaction study and self-diffusiophoretic Janus particle measurement of liquid phase adsorption isotherms provide evidence that the adsorption of formate, and by extension, the transfer hydrogenation reaction, may be tuned by the addition of an alcohol cosolvent. At low formate concentration, the cosolvent can serve to increase the reaction rate by increasing formate adsorption, yet at higher concentrations the presence of alcohol cosolvents can inhibit the reaction by saturating the surface with formate, thereby preventing adsorption of any substrate to be hydrogenated. As water–alcohol mixtures are commonly used in the hydrothermal liquefaction of lignocellulose, the results directly inform efforts to upgrade raw bio-oil *via* transfer hydrogenation with formates.

## Conclusions

We report a combined study demonstrating the ability of alcohol–water cosolvent mixtures to "tune" a Pd-catalyzed transfer hydrogenation reaction utilizing formate as the hydrogen source. Addition of alcohol cosolvent resulted in a shift of the maximum reaction rate to lower formate concentration. The changes in reaction rate were attributed to cosolvent tuning of formate adsorption onto the surface by increasing the dissolved formate activity. Quantitative measurement of formate adsorption onto Pt in pure water and a 20 mol% isopropyl alcohol cosolvent mixture showed a substantial increase in formate adsorption upon addition of the alcohol cosolvent. The findings provide a framework for solvent selection in transfer hydrogenation reactions and more broadly point to a strategy for tuning the solute adsorption in liquid phase catalytic reactions by the rational design of cosolvent mixtures.

## Data availability

Some of the data supporting this article are in the ESI.† Complete datasets will be placed on the CU Scholar repository at **https://scholar.colorado.edu**.

## Author contributions

Ezra A. Baghdady: conceptualization, methodology, investigation, formal analysis, writing – original draft, visualization, software. J. Will Medlin: conceptualization, methodology, supervision, funding acquisition. Daniel K. Schwartz: conceptualization, methodology, supervision, funding acquisition.

## Conflicts of interest

The authors declare no competing financial interest.

## Acknowledgements

This work was supported by the Department of Energy Office of Science, Basic Energy Sciences Program, Chemical Sciences, Geosciences, and Biosciences Division (Grant DE-SC-0005239). The imaging work was performed at the BioFrontiers Institute Advanced Light Microscopy Core (RRID: SCR_018302). Microscopy was performed on a Nikon Ti-E microscope supported by the Howard Hughes Medical Institute. This research was also supported in part by the Colorado Shared Instrumentation in Nanofabrication and Characterization (COSINC).

## References

1 D. Wang and D. Astruc, The Golden Age of Transfer Hydrogenation, *Chem. Rev.*, 2015, **115**(13), 6621–6686, DOI: **10.1021/acs.chemrev.5b00203**.

2 S. Moret, P. J. Dyson and G. Laurenczy, Direct Synthesis of Formic Acid from Carbon Dioxide by Hydrogenation in Acidic Media, *Nat. Commun.*, 2014, **5**, 1–8, DOI: **10.1038/ncomms5017**.

3 W. Leitner, Carbon Dioxide as a Raw Material: The Synthesis of Formic Acid and Its Derivatives from CO2, *Angew. Chem., Int. Ed. Engl.*, 1995, **34**(20), 2207–2221, DOI: **10.1002/anie.199522071**.

4 H. P. Reddy Kannapu, C. A. Mullen, Y. Elkasabi and A. A. Boateng, Catalytic Transfer Hydrogenation for Stabilization of Bio-Oil Oxygenates: Reduction of p-Cresol and Furfural over Bimetallic Ni-Cu Catalysts Using Isopropanol, *Fuel Process. Technol.*, 2015, **137**, 220–228, DOI: **10.1016/j.fuproc.2015.04.023**.

5 R. Nie, Y. Tao, Y. Nie, T. Lu, J. Wang, Y. Zhang, X. Lu and C. C. Xu, Recent Advances in Catalytic Transfer Hydrogenation with Formic Acid over Heterogeneous Transition Metal Catalysts, *ACS Catal.*, 2021, **11**(3), 1071–1095, DOI: **10.1021/acscatal.0c04939**.

6 J. K. Kenny, S. R. Neefe, D. G. Brandner, M. L. Stone, R. M. Happs, I. Kumaniaev, W. P. Mounfield, A. E. Harman-Ware, K. M. Devos, T. H. Pendergast, J. W. Medlin, Y. Román-Leshkov and G. T. Beckham, Design and Validation of a High-Throughput Reductive Catalytic Fractionation Method, *JACS Au*, 2024, **4**(6), 2173–2187, DOI: **10.1021/jacsau.4c00126**.

7 N. Akiya and P. E. Savage, Role of Water in Formic Acid Decomposition, *AIChE J.*, 1998, **44**(2), 405–415, DOI: **10.1002/aic.690440217**.

8 D. Zhang, F. Ye, T. Xue, Y. Guan and Y. M. Wang, Transfer Hydrogenation of Phenol on Supported Pd Catalysts Using Formic Acid as an Alternative Hydrogen Source, *Catal. Today*, 2014, **234**, 133–138, DOI: **10.1016/j.cattod.2014.02.039**.

9 N. Singh and C. T. Campbell, A Simple Bond-Additivity Model Explains Large Decreases in Heats of Adsorption in Solvents Versus Gas Phase: A Case Study with Phenol on Pt(111) in Water, *ACS Catal.*, 2019, **9**(9), 8116–8127, DOI: **10.1021/acscatal.9b01870**.

10 N. S. Gould, S. Li, H. J. Cho, H. Landfield, S. Caratzoulas, D. Vlachos, P. Bai and B. Xu, Understanding Solvent Effects on Adsorption and Protonation in Porous Catalysts, *Nat. Commun.*, 2020, **11**(1), 1–13, DOI: **10.1038/s41467-020-14860-6**.

11 A. Vittadini, A. Selloni, F. P. Rotzinger and M. Grätzel, Formic Acid Adsorption on Dry and Hydrated TiO2 Anatase(101) Surfaces by DFT Calculations, *J. Phys. Chem. B*, 2000, **104**(6), 1300–1306, DOI: **10.1021/jp993583b**.

12 T. L. Silbaugh, E. M. Karp and C. T. Campbell, Energetics of Formic Acid Conversion to Adsorbed Formates on Pt(111) by Transient Calorimetry, *J. Am. Chem. Soc.*, 2014, **136**(10), 3964–3971, DOI: **10.1021/ja412878u**.

13 Z. Zhang, X. Wang, J. Ma, R. Bian, H. Sui, L. He and X. Li, Measurement and Correlation of Solubility of Calcium Formate (Form α) in Different Binary Solvent Mixtures at Temperatures from 283.15 to 323.15 K, *J. Chem. Eng. Data*, 2019, **64**(6), 2475–2483, DOI: **10.1021/acs.jced.9b00009**.

14 B. Hu, X. Li, W. Busser, S. Schmidt, W. Xia, G. Li, X. Li and B. Peng, The Role of Nitrogen-Doping in the Catalytic Transfer Hydrogenation of Phenol to Cyclohexanone with Formic Acid over Pd Supported on Carbon Nanotubes, *Chem. – Eur. J.*, 2021, **27**(42), 10948–10956, DOI: **10.1002/chem.202100981**.

15 Z. Wang and H. Wang, Pt, Pd, and Rh Nanoparticles Supported on Polydopamine Nanospheres as Catalysts for Transfer Hydrogenolysis, *ACS Appl. Nano Mater.*, 2022, **5**(8), 11797–11808, DOI: **10.1021/acsanm.2c02798**.

16 E. A. Baghdady, J. W. Medlin and D. K. Schwartz, Enhancing the Self-Propelled Motion of Hydrogen Peroxide Fueled Active Particles with Formic Acid and Other Oxygen Scavengers, *Langmuir*, 2024, **40**, 21097–21105, DOI: **10.1021/acs.langmuir.4c02482**.

17 H. G. Schmidt, Safe Piranhas: A Review of Methods and Protocols, *ACS Chem. Health Saf.*, 2022, **29**(1), 54–61, DOI: **10.1021/acs.chas.1c00094**.

18 M. C. Jung, H. Kim, M. Han, W. Jo and D. C. Kim, X-Ray Photoelectron Spectroscopy Study of Pt-Oxide Thin Films Deposited by Reactive Sputtering Using O2/Ar Gas Mixtures, *Jpn. J. Appl. Phys., Part 1*, 1999, **38**(8), 4872–4875, DOI: **10.1143/jjap.38.4872**.

19 E. Kertalli, J. C. Schouten and T. A. Nijhuis, Effect of Hydrogen and Propylene on the Hydrogen Peroxide Decomposition over Pt, PtO and Au Catalysts, *Appl. Catal., A*, 2017, **538**, 131–138, DOI: **10.1016/j.apcata.2017.03.023**.

20 J. R. Howse, R. A. L. Jones, A. J. Ryan, T. Gough, R. Vafabakhsh and R. Golestanian, Self-Motile Colloidal Particles: From Directed Propulsion to Random Walk, *Phys. Rev. Lett.*, 2007, **99**(4), 8–11, DOI: **10.1103/PhysRevLett.99.048102**.

21 B. Greydanus, M. Saleheen, H. Wu, A. Heyden, J. W. Medlin and D. K. Schwartz, Probing Surface-Adsorbate Interactions through Active Particle Dynamics, *J. Colloid Interface Sci.*, 2022, **614**, 425–435, DOI: **10.1016/j.jcis.2022.01.053**.

22 M. J. Rice and C. A. Kraus, Conductance and Viscosity of Concentrated Aqueous Salt Solutions at 50.5°, *Proc. Natl. Acad. Sci. U. S. A.*, 1953, **39**(8), 802–811, DOI: **10.1073/pnas.39.8.802**.

23 B. W. J. Chen and M. Mavrikakis, Formic Acid: A Hydrogen-Bonding Cocatalyst for Formate Decomposition, *ACS Catal.*, 2020, **10**(19), 10812–10825, DOI: **10.1021/acscatal.0c02902**.
24 C. Kim, K. Lee, I.-H. Yoo, Y.-J. Lee, S. Ramadhani, H. Sohn, S. W. Nam, J. Kim, Y. Kim and H. Jeong, Strategy for Efficient H2 Production from a Mixture of Formic Acid and Formate Using Operando pH Measurements, *ACS Sustainable Chem. Eng.*, 2022, **10**(2), 888–898, DOI: **10.1021/acssuschemeng.1c06603**.
25 X. Xu, J. Luo, L. Li, D. Zhang, Y. Wang and G. Li, Unprecedented Catalytic Performance in Amine Syntheses: Via Pd/g-C3N4 Catalyst-Assisted Transfer Hydrogenation, *Green Chem.*, 2018, **20**(9), 2038–2046, DOI: **10.1039/c8gc00144h**.
26 M. K. Anwer, D. B. Sherman, J. G. Roney and A. F. Spatola, Applications of Ammonium Formate Catalytic Transfer Hydrogenation. 6. Analysis of Catalyst, Donor Quantity, and Solvent Effects upon the Efficacy of Dechlorination, *J. Org. Chem.*, 1989, **54**(6), 1284–1289, DOI: **10.1021/jo00267a012**.
27 J. Feng, C. Yang, D. Zhang, J. Wang, H. Fu, H. Chen and X. Li, Catalytic Transfer Hydrogenolysis of α-Methylbenzyl Alcohol Using Palladium Catalysts and Formic Acid, *Appl. Catal., A*, 2009, **354**(1–2), 38–43, DOI: **10.1016/j.apcata.2008.11.008**.
28 W. Song, N. Martsinovich, W. M. Heckl and M. Lackinger, Born-Haber Cycle for Monolayer Self-Assembly at the Liquid-Solid Interface: Assessing the Enthalpic Driving Force, *J. Am. Chem. Soc.*, 2013, **135**(39), 14854–14862, DOI: **10.1021/ja407698t**.
29 G. Li, B. Wang and D. E. Resasco, Solvent Effects on Catalytic Reactions and Related Phenomena at Liquid-Solid Interfaces, *Surf. Sci. Rep.*, 2021, **76**(4), 100541, DOI: **10.1016/j.surfrep.2021.100541**.
30 Q. Luo, G. Feng, M. Beller and H. Jiao, Formic Acid Dehydrogenation on Ni(111) and Comparison with Pd(111) and Pt(111), *J. Phys. Chem. C*, 2012, **116**(6), 4149–4156, DOI: **10.1021/jp209998r**.
31 J. E. Crowell, E. L. Garfunkel and G. A. Somorjai, The Coadsorption of Potassium and Co on the Pt(111) Crystal Surface: A TDS, HREELS and UPS Study, *Surf. Sci.*, 1982, **121**(2), 303–320, DOI: **10.1016/0039-6028(82)90045-0**.
32 I. T. McCrum and M. J. Janik, pH and Alkali Cation Effects on the Pt Cyclic Voltammogram Explained Using Density Functional Theory, *J. Phys. Chem. C*, 2016, **120**(1), 457–471, DOI: **10.1021/acs.jpcc.5b10979**.
33 R. Sang, C. A. M. Stein, T. Schareina, Y. Hu, A. Léval, J. Massa, V. Turan, P. Sponholz, D. Wei, R. Jackstell, H. Junge and M. Beller, Development of a Practical Formate/Bicarbonate Energy System, *Nat. Commun.*, 2024, **15**(1), 1–9, DOI: **10.1038/s41467-024-51658-2**.
34 S. Rajagopal and A. F. Spatola, Mechanism of Palladium-Catalyzed Transfer Hydrogenolysis of Aryl Chlorides Hy Formate Salts, *J. Org. Chem.*, 1995, **60**(5), 1347–1355, DOI: **10.1021/jo00110a045**.
35 A. H. Jenkins and J. W. Medlin, Controlling Heterogeneous Catalysis with Organic Monolayers on Metal Oxides, *Acc. Chem. Res.*, 2021, **54**(21), 4080–4090, DOI: **10.1021/acs.accounts.1c00469**.
36 T. L. Silbaugh, E. M. Karp and C. T. Campbell, Energetics of Methanol and Formic Acid Oxidation on Pt(111): Mechanistic Insights from Adsorption Calorimetry, *Surf. Sci.*, 2016, **650**, 140–143, DOI: **10.1016/j.susc.2015.12.008**.
37 G. Li, Z. Zhao, T. Mou, Q. Tan, B. Wang and D. Resasco, Experimental and Computational Kinetics Study of the Liquid-Phase Hydrogenation of C C and C O Bonds, *J. Catal.*, 2021, **404**, 771–785, DOI: **10.1016/j.jcat.2021.09.002**.
38 J. K. Kenny, D. G. Brandner, S. R. Neefe, W. E. Michener, Y. Román-leshkov, G. T. Beckham and J. W. Medlin, Catalyst Choice Impacts Aromatic Monomer Yields and Selectivity in Hydrogen-Free Reductive Catalytic Fractionation, *React. Chem. Eng.*, 2022, **7**(7), 2527–2533, DOI: **10.1039/d2re00275b**.
39 D. G. Brandner, J. S. Kruger, N. E. Thornburg, G. G. Facas, J. K. Kenny, R. J. Dreiling, A. R. C. Morais, T. Renders, N. S. Cleveland, R. M. Happs, R. Katahira, T. B. Vinzant, D. G. Wilcox, Y. Román-Leshkov and G. T. Beckham, Flow-through Solvolysis Enables Production of Native-like Lignin from Biomass, *Green Chem.*, 2021, **23**(15), 5437–5441, DOI: **10.1039/D1GC01591E**.

 